Experimental and numerical investigation of gap K-joints of rectangular hollow section trusses

Slimani, F., Benzerara, M. & Saidani, M

DOI 10.3221/IGF-ESIS.62.08
ISSN 1971-8993

Publisher: Gruppo Italiano Frattura

Visual Abstract

Experimental and numerical investigation of gap K-joints of rectangular hollow section trusses

Faycal Slimani
Civil Engineering Laboratory, Badji Mokhtar- Annaba University, P. O. Box 12, 23000 Annaba, Algeria
faycal.slimani@univ-annaba.dz;slimani_faycal@yahoo.fr

Mohammed Benzerara
Materials, Geomaterials and Environment Laboratory, Department of Civil Engineering, Badji Mokhtar- Annaba University, P. O. Box 12, 23000 Annaba, Algeria
Civil Engineering Laboratory, Badji Mokhtar- Annaba University, P. O. Box 12, 23000 Annaba, Algeria
mohammed.benzerara@univ-annaba.dz;mohammed.benzerara@yahoo.com

Messaoud Saidani
Faculty of Engineering and Computing, Coventry University, Priory Street,Coventry CV1 5FB, UK
m.saidani@coventry.ac.uk

ABSTRACT. This paper is concerned with investigating the plastic behavior of gap K-joints of truss girders, made from thin-walled rectangular hollow section members. The novelty of the method is that it offers a rigorous numerical model that may be generalized to cover similar joints with different parameters to the one covered in this study. An experimental study was carried out on a full-scale girder under concentrated load on two central nodes. A numerical analysis was carried out using ABAQUS to investigate the behavior of this type of joints and comparison is made with the experimental results. The study aims to examine and define the analytical model for this type of joints. The results obtained show that sections with chord/brace thickness ratio (t_0/t_1)=1 exhibit a different behavior compared to sections with (t_0/t_1)>1. From this study, it was possible to obtain the modes of failure of such sections followed by a comparative study on the determination of the joint capacity using Eurocode 3 and CIDECT.

KEYWORDS. Rectangular hollow section; Gap joint; Lattice girder; Plasticity; Finite element modeling.

OPEN ACCESS

Citation: Slimani, F., Benzerara, M., Saidani, M., Experimental and numerical investigation of gap K-joints of rectangular hollow section trusses, Frattura ed Integrità Strutturale, xx (2022) 107-125.

Received: 09.04.2022
Accepted: 01.08.2022
Online first: 10.08.2022
Published: 01.10.2022

INTRODUCTION

Rectangular hollow sections have continued to be the subject of numerous studies, analytical, experimental and theoretical [1–4]. The behavior of K-joints with a hollow rectangular section is complex as it has too many influential parameters [5–8]. When designing the chords, the resulting moments due to eccentricity in the joint must be taken into account. When assuming that all members are pin-connected, these "eccentricity moments" can be easily overlooked. Moreover, the Canadian HSS Design Guide [9] states that connections are to be designed within a certain range of validity, however, for cases where $L/h < 6$, these secondary moments need to be considered.
Frater and Packer [10] showed that the bending moments in the chords obtained from experimental results of large-scale gap-jointed RHS trusses gave poor numerical agreement; it seems therefore necessary to use a rigorous method to predict the maximum bending moment and verify its interaction with the maximum axial force. The large deformations of the chord face are usually present in RHS truss connections and these contribute to the distributions of axial force and bending moments. Coutie and Saidani [11, 12] showed that by simulating the deformations in the faces of the chords, the experimental behavior of the truss could be reproduced by theoretical models.
A numerical analysis conducted by Kim and Lee [10] on the behavior of rectangular hollow section (RHS) joints with a bracing-to-chord width ratio $\beta=1$ showed that lateral instability could easily occur. This phenomenon has been found to significantly alter the strength of the joint. Therefore, and following simple mechanics, an analytical and more rational expression of the width ratio has been proposed and validated.
The majority of research work on gap K-joints with rectangular hollow section has been carried out on sections of 100 mm x 100 mm with chord/brace thickness ratio of $t_0/t_1>1$.Based on these studies, a contribution of this research is to carry out a comparative study for a better understanding of the behavior of joints of rectangular hollow sections, with a smaller section of 70 mm x 50 mm and chord/brace thickness ratio of $t_0/t_1=1$.This paper deals with an experimental investigation of the behavior of gap K-joint of rectangular hollow section and assessing the deformations obtained during the experiment. Stresses, axial forces and bending moments are determined. A numerical simulation using the Abaqus software was also carried out for an in-depth analysis and validation of the results obtained from the experimental study.

EXPERIMENTAL SETUP

A full scale truss girder made of steel S235 and gapped K-joints is tested. It has a symmetrical shape with respect to its center. The experiment was carried out on a test slab with a gantry fitted with two hydraulic jacks with a maximum capacity of 20 t (200 kN) each.

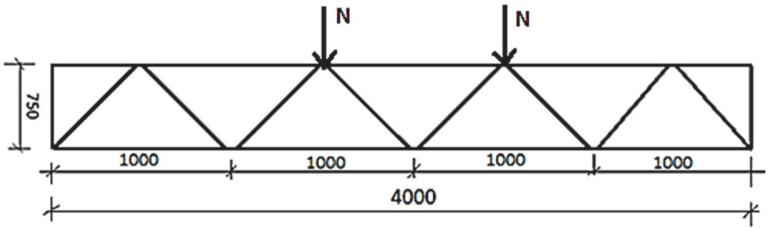

Figure 1: Design of truss.

Settings	Total length	Total height	Chords	Bracings
Unit (mm)	4000	750	70x50x2.5	60x30x2.5

Table 1: Dimensions and sections of the elements.

The main mechanical and geometric characteristics of the specimen were provided by the manufacturer. These can be
E: Young's modulus = 210 GPa
A_c: Cross-sectional area of chord = 575 mm^2
A_d: Cross-sectional area of diagonal = 425 mm^2

Protocols and experimental devices

The beam is mounted on a test slab, the load is distributed at the two central nodes through a rigid steel H profile. A wind-bracing system has been adopted to ensure the out-of-plane stability of the truss (Fig 2).

Figure 2: Truss test.

Geometric characteristics of the truss

Analytical models are used to study the effect of the main parameters and describe the behaviour of joints. However, taking all the parameters into account leads to a model that is far too complicated. For this reason, various simplified models are used depending on the mode of failure analysed, and in combination with results of laboratory assembly tests, these models make it possible to establish sizing equations. As the design and sizing of a structure always result from compromises between resistances, stability, manufacturing cost and maintenance, these can sometimes be conflicting.

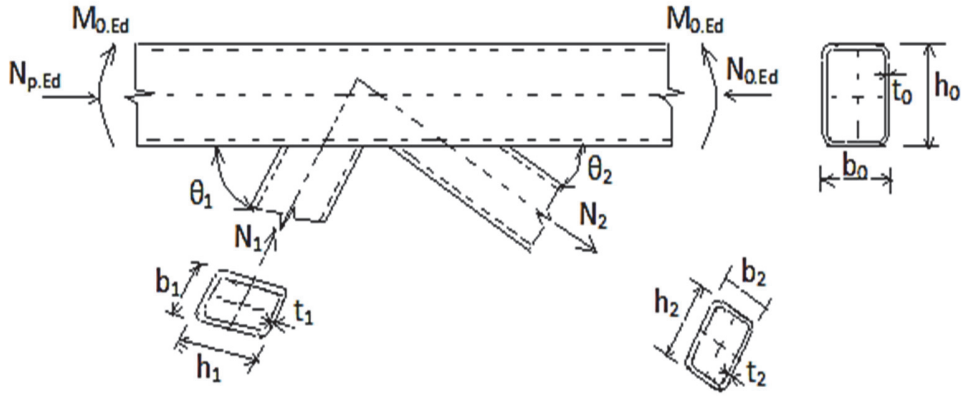

Figure 3: Geometric characteristics.

Truss	Joint type	θ_1	θ_2	β	b_0/t_0	b_1/t_1	t_0/t_1	b_1/b_2
T	Gap-joint	60.6	60.6	0.9	20	12	1.0	1.0

Table 2: Different parameters of the joint.

Instrumentation and measurement

Electrical Resistance Strain Gauges were placed on the four faces of the elements constituting the joint (Figs. 4 and 5), in order to measure the strains and subsequently determine the stresses. Then, the measured values were converted into forces and bending moments in the braces and in the chord.

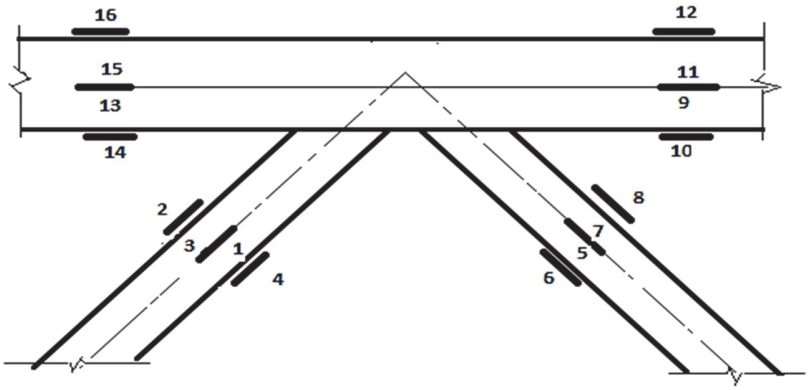

Figure 4: Attachment and numbering of gauges.

Figure 5: Attachment of gauges.

Reinforcement has been adopted at the level of the supports and the joints under the applied load location in order to avoid the rapid deformations of the side walls of the chord as shown in (Figs. 2 and 5).

TEST RESULTS

The main parameters (Tab.2) influencing the joint behavior of hollow rectangular section trusses are: the chord width/thickness ratio (b_0/t_0), the truss width/thickness ratio bj/tj, and the angle of the braces with the chord (θ). All these parameters have been the subject of previous research work [4,8,11]. Based on the results, and with a ratio of $t_0/t_1>1$ it was found that these parameters cause deformations on the face of the chord without affecting the web. In the present work, two parameters were the exception with respect to the investigations carried out, the chord/brace thickness ratio $t_0/t_1=1$, which should be $t_0/t_1>1$, and coefficient β which must be ≤0.85 as recommended for K-joints [12]. These parameters were the cause of the buckling of the chord wall. One test was enough to show this particularity. More tests would have been desirable, but they are very costly to execute, hence the use of results from the literature and the numerical modeling carried out in this study are proposed to overcome this shortcoming.
The study consists in close examination of the joints under the loading, whose chord will be the most stressed by the loading from the diagonals.

Distribution of axial forces

The axial force (Fig. 3) was evaluated for each member using the equation given below. The axial force in element i according to Saidani [8] may be written as follows (there are 4 strain gauges at each section, hence n=4):

$$N_i = \sum_{i=1}^{4} \varepsilon_i \cdot E \cdot A = \frac{(\varepsilon_1 + \varepsilon_2 + \varepsilon_3 + \varepsilon_4)}{4} \cdot E \cdot A \quad (1)$$

E: Young's modulus.
A: The cross-sectional area of member.
ε_i: Strain.
The variation of the axial force in the braces (branches) with respect to the loading was approximately linear up to the ultimate load of 50 kN (Fig. 6).

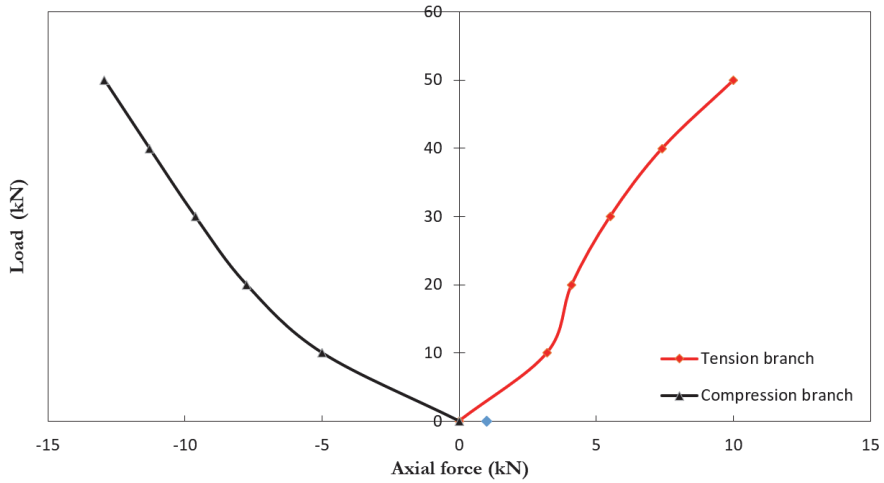

Figure 6: Diagram Load/axial force in the branch.

The values of the axial forces calculated from the deformations in the brace of the joint are shown in the Tab.3.

Load (kN)	Axial forces (kN)	
	Compression branch	Tension branch
0	0	0
10	-5.0	2.5
20	-7.1	4.1
30	-9.2	5.0
40	-11.3	7.0
50	-12.9	10.2

Table 3: Axial forces in branches.

Stress distribution diagrams

The relationship between stress and local deformation was linear up to an applied load of 50 kN. Furthermore, the deformations recorded on the compression diagonal are clearly higher than those on the tension diagonal (Fig.7).
The stress and strain values in the brace of the joint are shown in Tab. 4.

The face chord deformation

The deformation was greatest at the joint where the axial force was highest. The instability occurred in all four sides of the chord section. This confirms the observations from previous investigations of tested joints. The deformations of the front wall (face) of the chord behaved linearly up to approximately a load of 20 kN (Fig. 8), however from this point onwards, the behavior was non-linear. This non-linearity appears to be caused by deformations and buckling of the sidewalls of the chord. The points on the curve (Fig. 8) correspond to the various loading levels see (Tab 5).

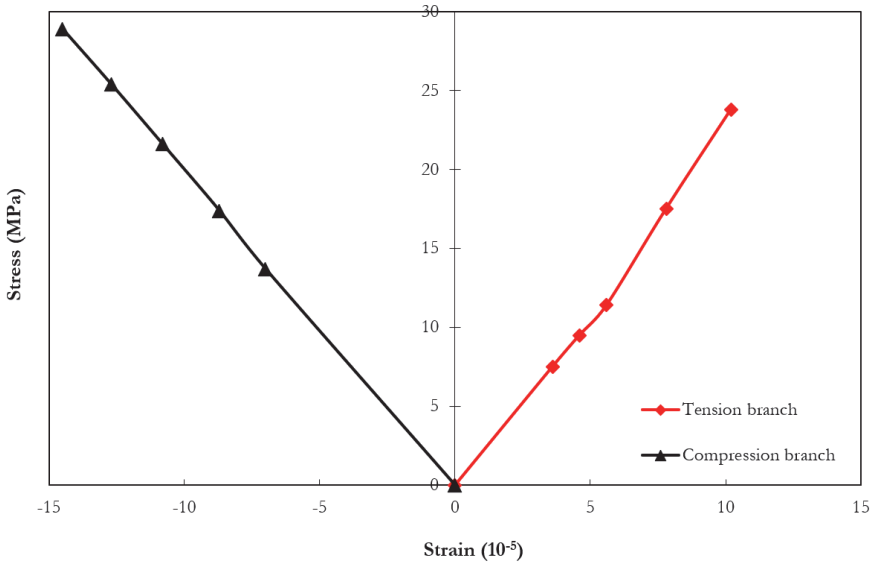

Figure 7: Stress-Straincurve in the branch.

Load (kN)	Stress (MPa)		Strain (10^{-5})	
	Tension branch	Compression branch	Tension branch	Compression branch
0	0	0	0	0
10	7.5	-13.9	3.6	-7.0
20	9.5	-17.4	4.6	-8.7
30	11.4	-21.6	5.6	-10.8
40	17.5	-25.4	7.8	-12.7
50	23.8	-28.9	10.2	-14.5

Table 4: Stress and Strain values in the branches.

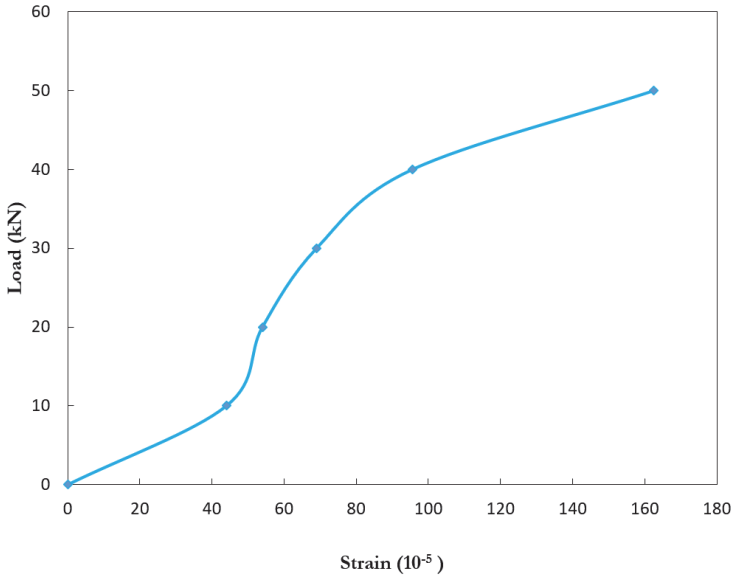

Figure 8: Load-Strain curve in the chord face.

The values of strain in the chord of the joint considered are mentioned in Tab.5.

Load (kN)	Strain (10^{-5})
0	0.0
10	44.0
20	54.0
30	69.0
40	95.5
50	162.4

Table 5: Strain in the chord face.

Deformation of the chord sidewalls

The load-strain curve of the sidewalls of the chord had a similar appearance to that of the face of the chord, except that their plasticization caused significant deformations resulting in a clearly visible buckling (Fig. 9).

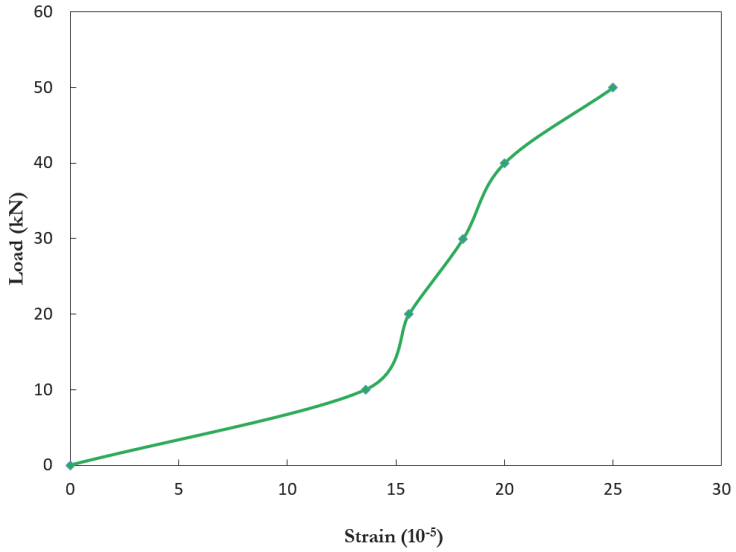

Figure 9: Load-Strain curve in sidewalls of the chord.

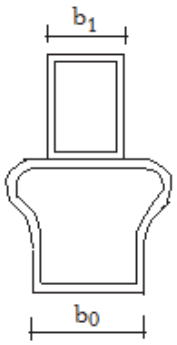

Figure 10: Deformation of the chord sidewalls.

Instability (buckling) of the side or web of the chord under the compression brace, generally only occurs when the brace/chord width ratio (β) is greater than about 0.85, more particularly when the coefficient β=1 [20] and the ratio between the width of the diagonal and the chord is equal to one (b_1/b_0=1). This ratio has a great influence on the

behavior of the joint, in particular, on the deformations of the walls of the chord. An optimal ratio proves to be essential on the resistance of the joint, therefore, reduced deformations (Fig. 10).
Based on the results obtained from the strain values (Tab. 6), a compromise must be established between the load and the dimensions of the elements, in order to limit the deformations of the sidewalls of the chord and to have a ratio β according to the standards of design [12].

Load (kN)	Strain (10^{-5})
0	0
10	13.6
20	15.6
30	18.1
40	20.0
50	25.0

Table 6: Strain values on the side walls of the chord.

NUMERICAL ANALYSIS

A numerical analysis using the commercial software ABAQUS was carried out in order to validate the experimental study [13–15]. The beam was created in 3D (Fig.11) and then analyzed. As these are thin hollow sections, the shell element seems to be the most suitable for this type of section. The calculation software gives the possibility to choose the number of nodes of the chosen element or it does it automatically. This approach made it possible to directly determine the values of strains, stresses, displacements and forces at any point within the structure [16–19].

Geometry and mesh

The shell element can be used effectively in a nonlinear analysis including investigation of plasticity, large displacement, and fracture. An adequate mesh represents a good compromise between calculation time and accuracy of the results.

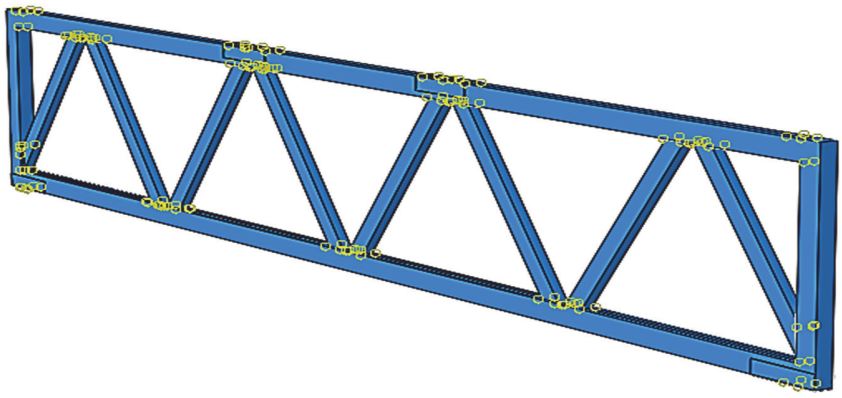

Figure 11: Overall view of the truss.

Loading and boundary conditions

The tested truss is simply supported on a hinge and a roller. The loading is applied on the two central nodes of the truss (Fig. 13).
The load is introduced as a pressure on the joint (Fig. 14).

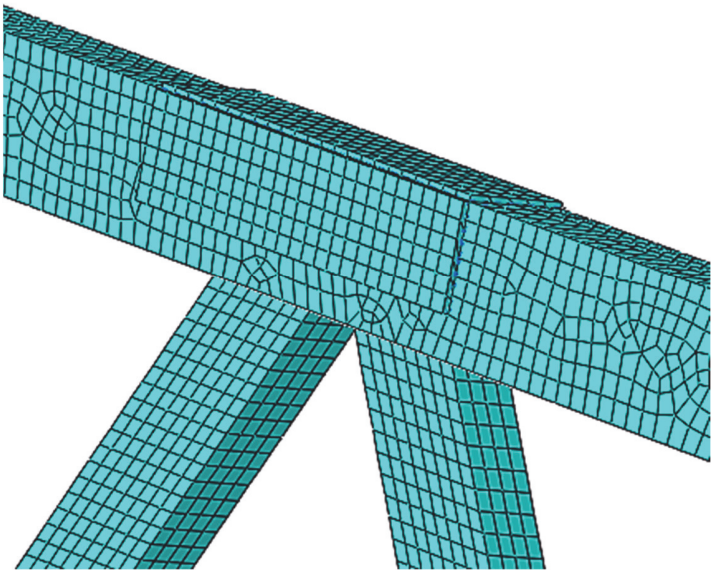

Figure 12: Joint mesh.

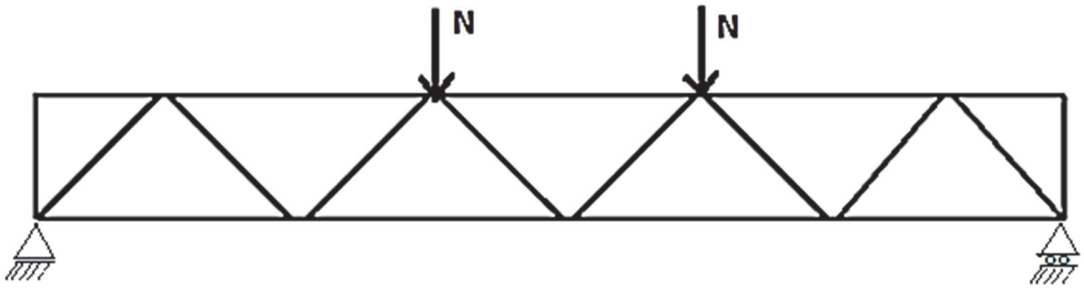

Figure 13: Supports of the beam.

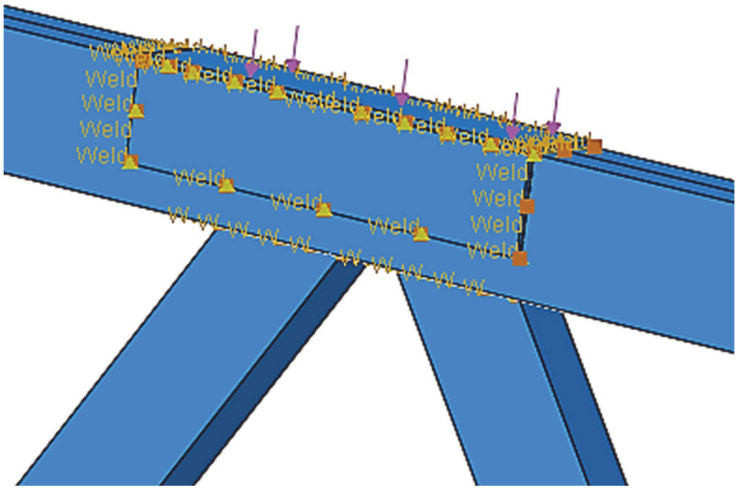

Figure 14: Joint load.

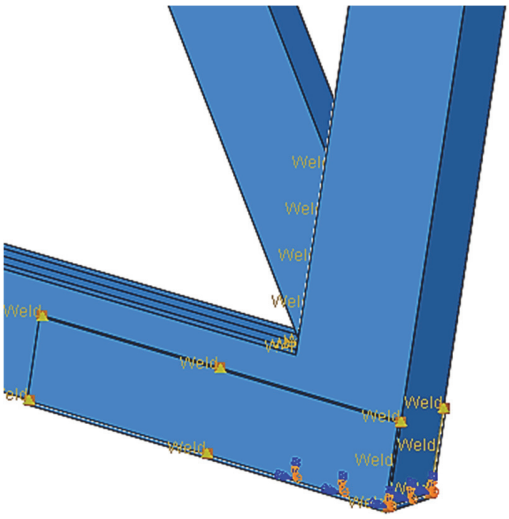

Figure 15: Boundary conditions.

Fig. 16 shows that the behaviour of the compressed diagonal was elastic and a convergence of the results obtained from the two approaches. Moreover, the average percentage error between the numerical and experimental analysis of strains is equal to 16.1%, respectively (Tab. 7 and Fig. 17). The difference are mainly due to the assumptions made regarding the material properties of specimen, the presence of residual stresses from the welding, as well as any inaccuracies in the testing set up, such boundary conditions, out-of-plane deformations however small, etc.

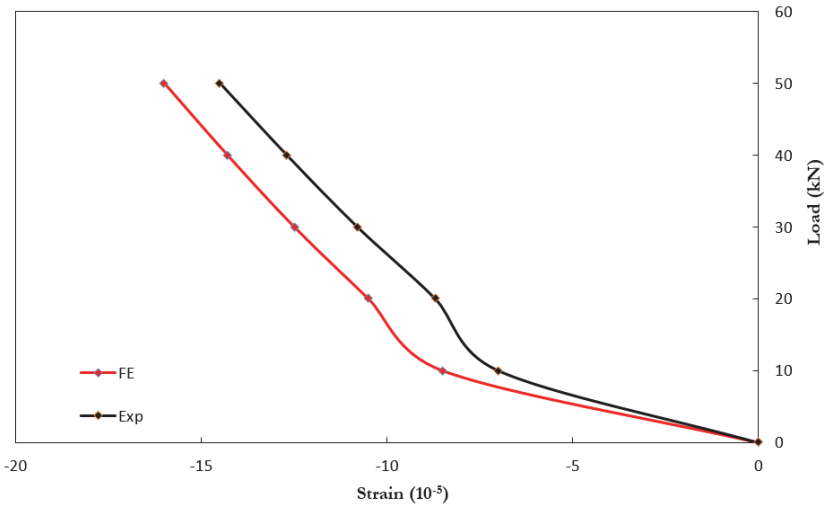

Figure 16: Load-Strain curvein the compression branches between numerical analysis (FE) and experimental (Exp).

Load (kN)	Compression branch Strain (10^{-5})		Percentage error (P) $\frac{(X_n - X_e)x100}{X_e}$
	Numerical	Experimental	Strain (%)
0	0	0	0
10	-8.5	-7.0	21.4
20	-10.5	-8.7	20.6
30	-12.5	-10.8	15.7
40	-14.3	-12.7	12.5
50	-16.0	-14.5	10.3

Table 7: Strain values in the compressed branches and percentage error between numerical analysis and test results.

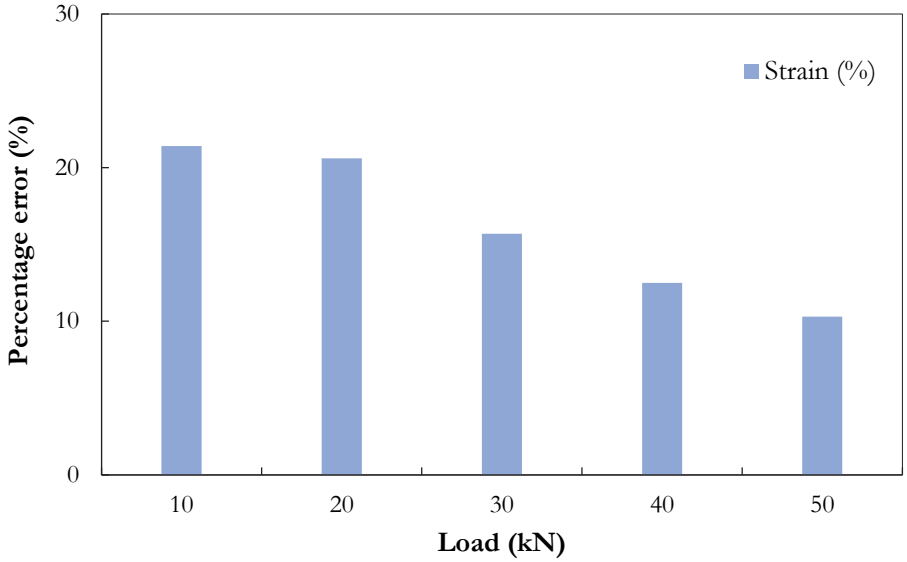

Figure 17: Percentage error between numerical analysis and experimental results.

Bending moment in the chord

According to Saidani[8], in lattice girders where the joints are gapped, the secondary moments can be quite large, and the bending moments in the chord may be obtained as follows [8]:

$$M_{10-12}^{i}=\frac{E\cdot Z}{2}\cdot\left(\varepsilon_{10}-\varepsilon_{12}\right) \tag{2}$$

M_{10-12}^{i} is the bending moment at the right end of the chord.

$$M_{14-16}^{i}=\frac{E\cdot Z}{2}\cdot\left(\varepsilon_{14}-\varepsilon_{16}\right) \tag{3}$$

M_{14-16}^{i} is the bending moment at the end of the chord.

$$Z=\frac{2I_{i}}{b_{i}}:\ \text{Elastic modulus of the member} \tag{4}$$

$$I_{i}=\left(\frac{b_{i}t_{i}^{3}}{6}\right)\cdot\left(4\alpha^{2}-12.72\alpha+11.946\right):\ \text{the second moment of area} \tag{5}$$

$$\alpha=\frac{b_{i}}{t_{i}} \tag{6}$$

Tab. 8 shows the values of bending moments at the left and the right ends of the joint, as well as the percentage errors between the experimental and numerical analysis.

The bending moment in the chord was predominantly in single curvature. It varies linearly with the applied load up to approximately a load of 40 kN (Fig. 19), however from this point onwards the behavior became on-linear. This variation in bending moment was related to local yielding of the chord face and its side walls.

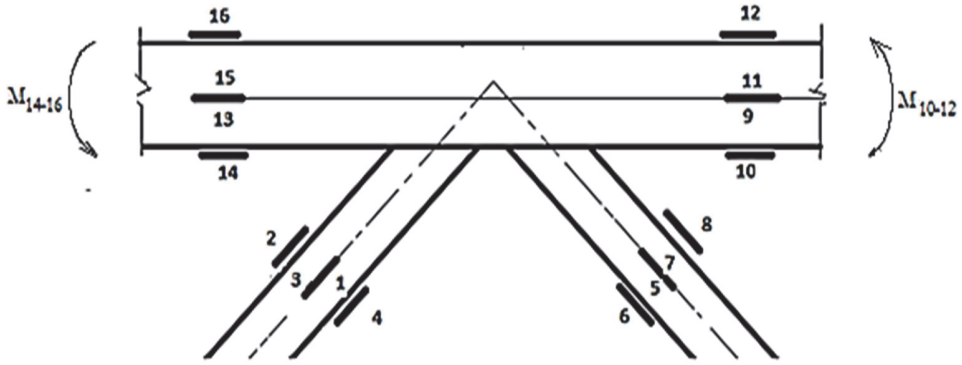

Figure 18: Notations for bending moments.

Load (kN)	Bending moment (kN.m)					
	Numerical		Experimental		Percentage error (P) $\frac{(X_n - X_e)x100}{X_e}$	
	M_{14-16}	M_{10-12}	M_{14-16}	M_{10-12}	P_{14-16}(%)	P_{10-12} (%)
0	0	0	0	0	0	0
10	-0.24	0.12	-0.19	0.09	26.3	33.3
20	-0.51	0.25	-0.38	0.20	34.2	25.0
30	-0.70	0.40	-0.58	0.35	20.6	14.2
40	-0.95	0.53	-0.75	0.45	26.6	17.7
50	-1.39	0.77	-1.10	0.68	26.3	13.2

Table 8: Bending moment and percentage error values in the chord between numerical analysis and experimental.

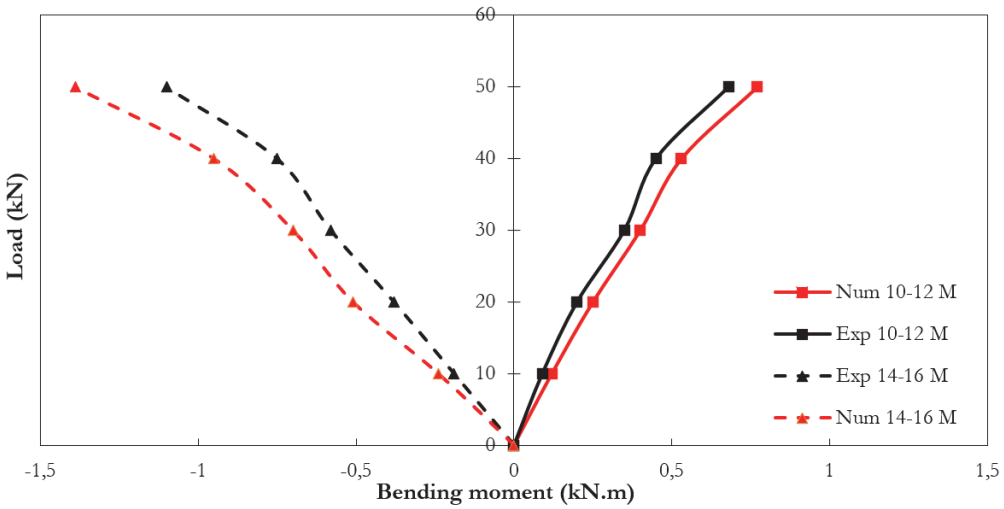

Figure 19: Load-Bending moment curvein the chord between numerical analysis and experimental.

The chord's bending moment results obtained from both approaches are expressed in the histogram with an average error percentage of 26.8% and 20.6% for the left and right joint moments (Fig.20).
In general, the origin of this error between numerical and experimental analysis is certainly due to certain failures which can occur at any level of loading during the course of the test, and especially for a four-point test, such as the protocol and the experimental devices, reliability of gauges, geometric imperfections, presence of the residual stresses, out-of-plane deformations however small, etc.

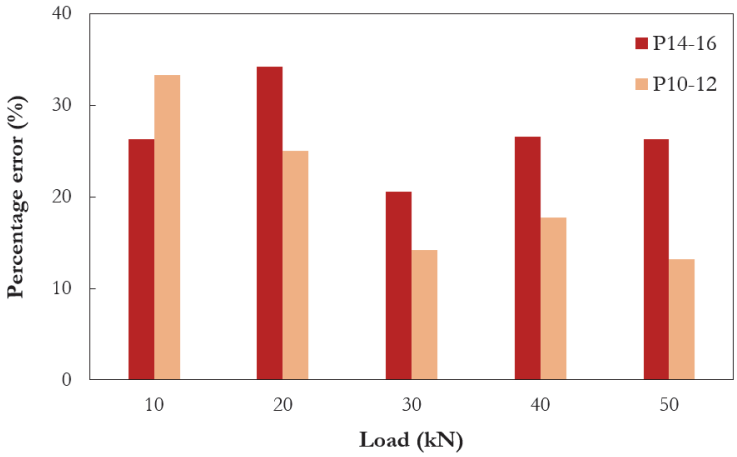

Figure 20: Percentage error between the two approaches.

Analytical models and failure modes

When the ratio b_0/t_0 or h_0/t_0 of the chord is large enough, the local buckling modes occur. According to Wardenier [1] two modes of failure could be used for the calculation of the resistance of connections, such as the yielding of the chord face. Many formulas exist in the literature; some have a theoretical basis but most are empirical or semi-empirical in nature for the various modes of failure. The general criterion is based on the ultimate strength concept. The CIDECT recommendations have been established so that the limit state of deformation under service loads is satisfied [12].

The factors used in the equations have been established and reflect the main strength parameters; namely the plastic capacity in bending ($f_{y0}.t_0^2/4$), ratio β, the slenderness ratio of the walls of the chord (ɣ), as well as the influence of the presence of compression force in the chord f(n).

The same deformations at the levels of the side walls and the face of the chord have been observed both through the numerical analysis and the experimental results (Figs. 21 to 25).

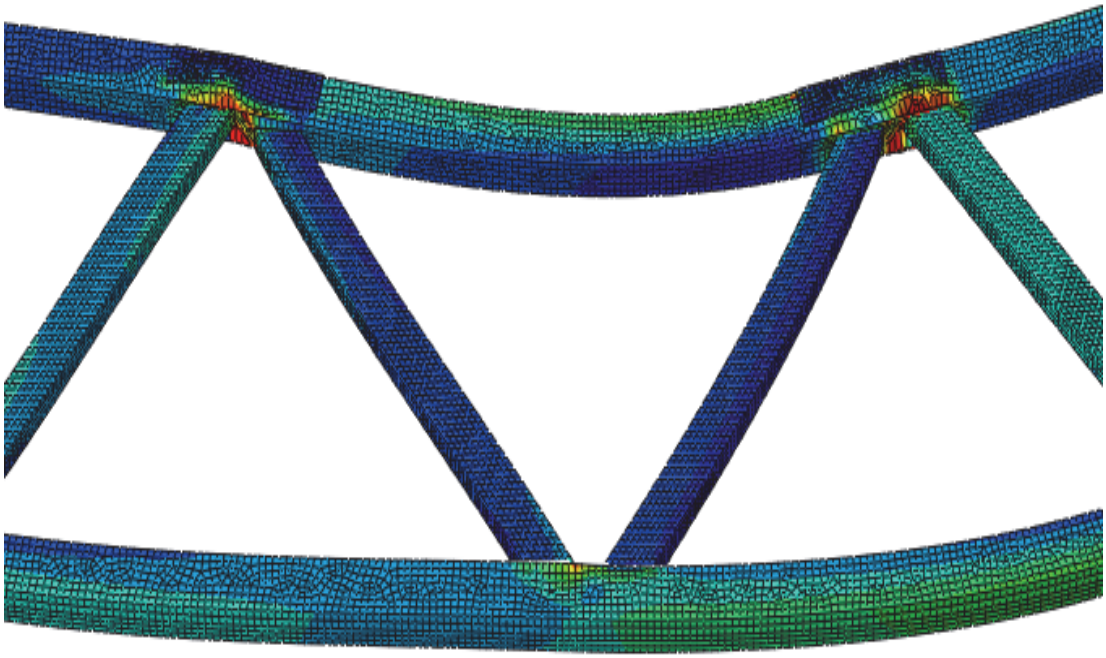

Figure 21: Plasticization of the central joints.

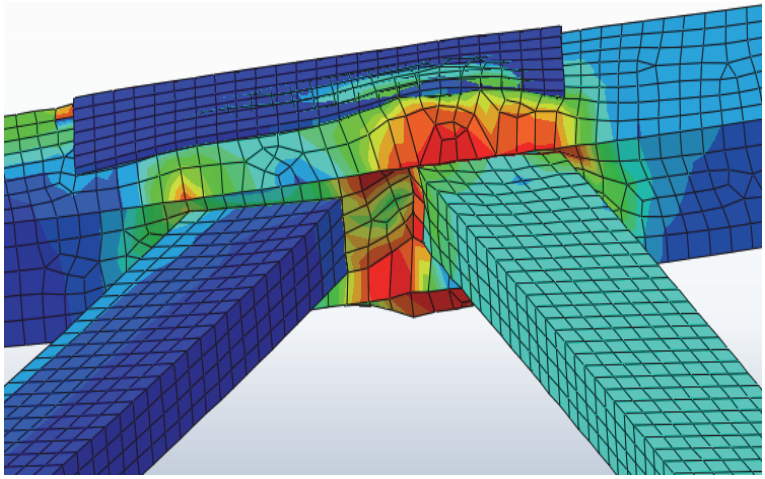

Figure 22: Right central joint failure (Numerical analysis).

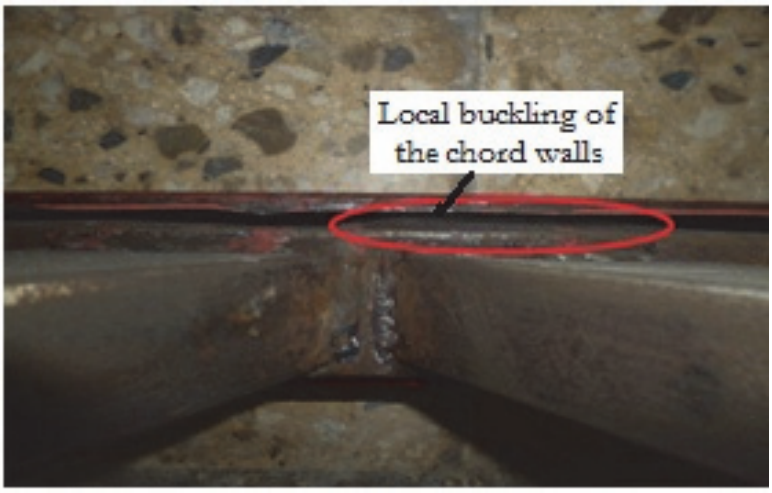

Figure 23: Right central joint failure (Experimental).

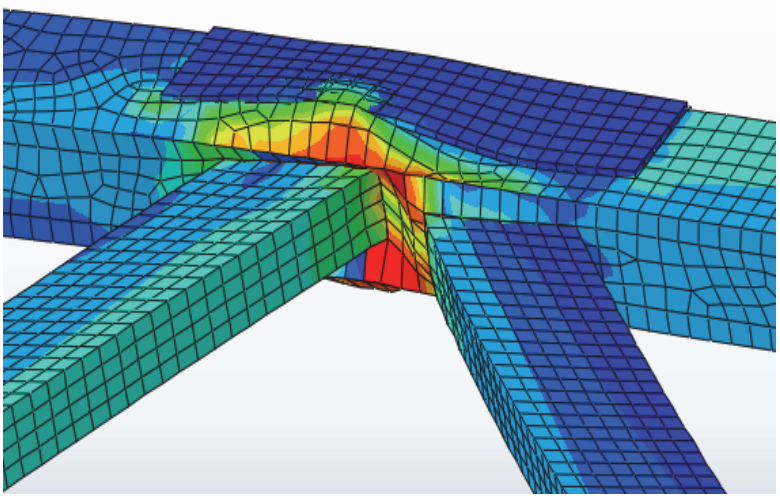

Figure 24: Left central joint failure (Numerical analysis).

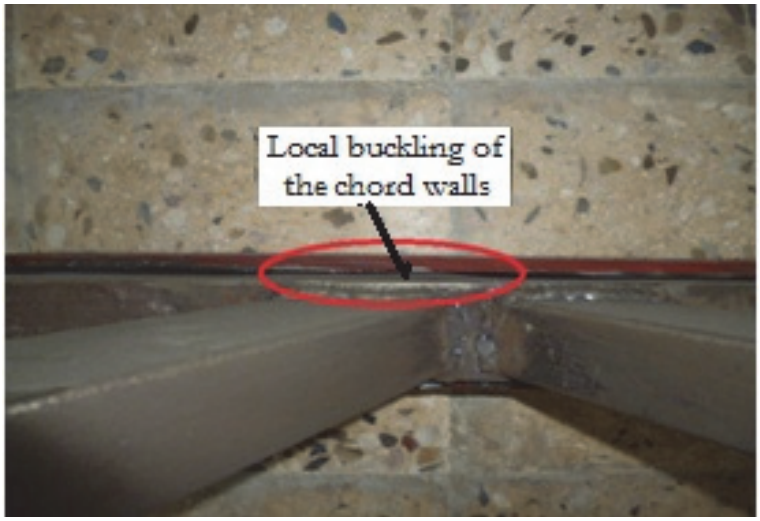

Figure 25: Left central joint failure (Experimental).

Effects of slenderness ratio on chord web

An additional numerical simulation is carried out on a range of values, aimed at observing the effect of the slenderness of the walls of the chord on the capacity of the joint. A variety of chord thickness values (Tab. 9) were chosen in order to observe the behavior of the chord web.

Load (kN)	Strain (10^{-5})			
0	0.0	0.0	0.0	0.0
10	5.03	3.78	2.9	2.48
20	10.1	7.56	5.9	4.97
30	16.0	11.3	8.9	7.4
40	26.1	15.8	12.0	9.83
50	57.6	22.4	15.3	12.2
t_0 (mm)	2,5	3	3,5	4
$\gamma = b_o/2t_0$	10	8.33	7.14	6.25

Table 9: Strain values in the web of the chord for different slenderness ratios.

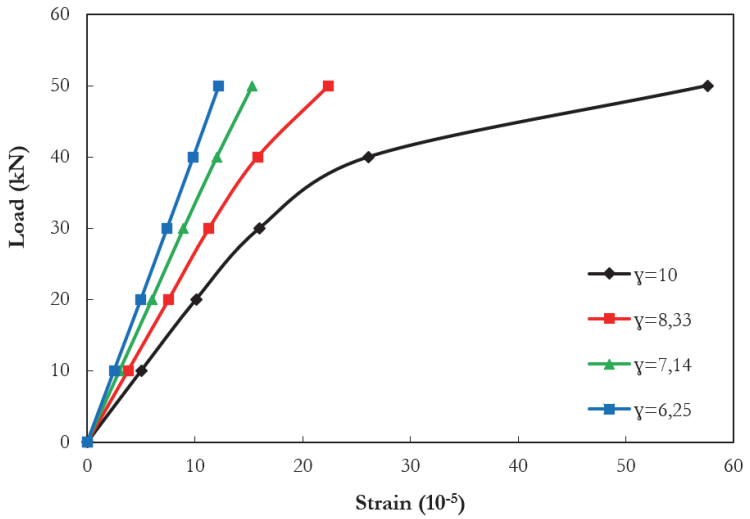

Figure 26: Load-Strain curve in chord sidewalls for different slenderness ratios.

The slenderness ratio has been an influential parameter on the deformations of the web of the chord and more particularly on the capacity of the joint. Fig. 26 shows that slenderness ratios of 6.25, 7.14 and 8.33 predict the elastic deformations of the chord web. The results provide good predictions of the joint capacity.

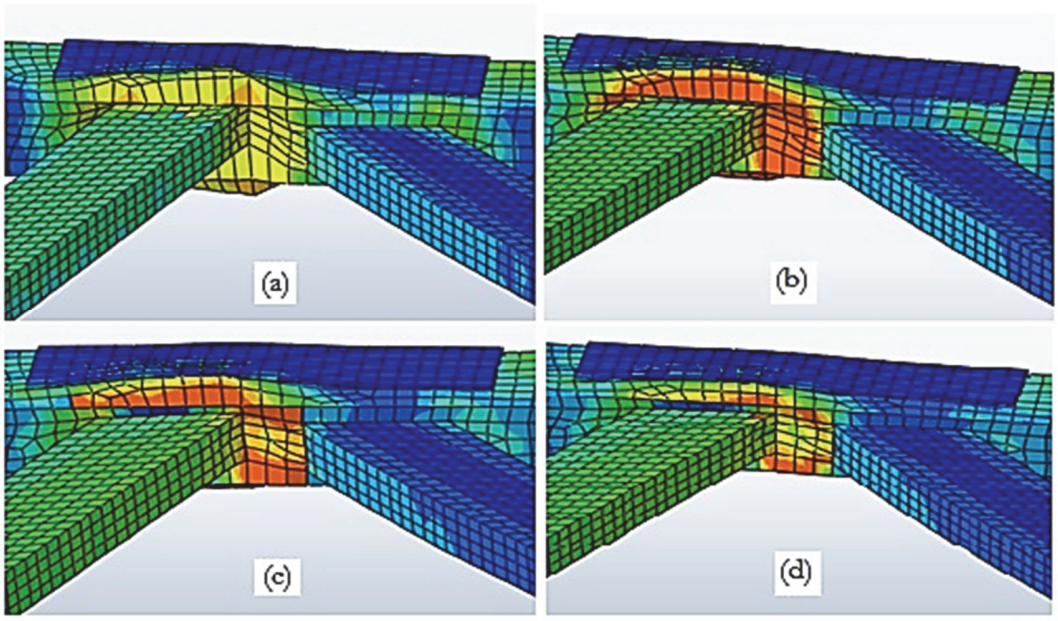

Figure 27: Plastification view of trusses with different slenderness ratios: (a) ɣ=10; (b) ɣ=8,33; (c) ɣ=7,14; (d) ɣ=6,25.

Standards	Failure	Joint capacity	Values (kN)
Eurocode	Chord face failure	$N_{i,RD} = \frac{8.9\sqrt{\gamma k_n f_{y0} t_0^2}}{\sin\theta_1}\left(\frac{b_1+b_2+h_1+h_2}{4b_0}\right)/\gamma_{MS}$ $\gamma = \frac{b_0}{2t_0}$ $k_n = 1.3 - \frac{0.4n}{\beta}$ $n = \frac{\sigma_{0,Ed}}{f_{y0}}$	42.7
CIDECT	Chord face failure	$N^*_i = 8.9\frac{f_{y0}t_0^2}{\sin\theta_1}.\left[\frac{b_1+b_2+h_1+h_2}{4b_0}\right].\sqrt{\gamma}.f(n)$ $f(n) = 1.3 + \frac{0.4n}{\beta}$	42.7

Table 10: Axial resistance of gap K-joint (joint capacity).

Joint capacity

Several numerical and experimental investigations have been carried out on the behavior of joints in rectangular hollow section trusses to established design standards and define the parameters influencing the resistance of joints and the relationships governing their resistance. The mechanical and geometrical parameters of the model are shown in (Fig. 3) and are used to calculate the joint capacity (Tab. 10).

As the sections of the truss elements are small, the values of k_n and f(n) are greater than one. According to CIDECT [12] and Eurocode 3 [20], these values must be less than or equal to one. Therefore, both approaches gave the same value of the joint strength. Nevertheless, up to the service load of 50 kN, the axial forces in the branches (Tab. 2) were lower than

the value of the joint capacity (42.7 kN). Except that and according to the load-strain curve in the chord (Fig.8), the capacity of the joint should be limited to a load of 40 kN, in order to limit the deformations of the walls of the chord.
No relationship has been given in the standards (CIDECT and Eurocode 3) to determine the resistance of the K-joint for hollow rectangular sections in the case of lateral buckling of the walls of the chords with β>0,85. In this study, the deformations of the sidewalls of the chord were predominant (Fig. 25). Gap K-joint trusses have a higher resistance if the branch to chord width ratio is as high as possible [12,20].

CONCLUSIONS

This work is a contribution with an alternative method to the classical means of studies of steel truss girders with hollow sections. Purely experimental methods are often very expensive when trusses are tested on a real scale, requiring special equipment. On the other hand, these experiments, which can turn out to be indicators, often provide more qualitative than quantitative results. A parametric study is necessary, but it can increase the cost and the time necessary for its realization.
From this investigation, the following may be concluded:

- Thin rectangular hollow section truss with thickness ratio between chord and braces $t_0/t_1=1$ exhibits slightly different behavior compared to trusses with thickness ratios $t_0/t_1>1$. This phenomenon of buckling of the chord walls has been observed even for thick sections. To prevent this buckling, the CIDECT recommendations require that this ratio is to be as high as possible.
- Given the thinness of the chord section, reinforcement by a U-profile of the joint at the point of application of the load is necessary but which unfortunately could not prevent plasticization of the sidewalls of the chord.
- Both approaches provided interesting results about the use of thin hollow rectangular sections. They have also shown that the major drawback is at the joint where the load is applied.
- As the sections of the truss elements are small, the CIDECT and Eurocode give the same values of the joint capacity.
- No relationship has been given in the literature on gap K-joint resistance in the case of lateral buckling of the chord walls. Whereas, in this work the deformations of the side walls of the chord were predominant.
- It is better to reinforce the section of the chord at the level of the joint where the loading is applied.
- The majority of past research work was carried out on three-point tests and with thickness ratios of the chord and the diagonals $t_0/t_1>1$, and a width ratio between the chord and the diagonals $\beta \leq 0.85$. The novel contribution of this work shows that the section with the thickness ratio $t_0/t_1=1$ and with $\beta=0.9$ gives considerable deformations of the web of the chord, therefore a buckling of the walls.
- A complementary numerical simulation is carried out on a range of values of the slenderness ratio of the web of the chord, has shown the important effect of this ratio on the walls of the chord. Moreover, this ratio of slenderness influences the capacity of the joint as well as the failure mode.
- It was found that, despite the very high stresses that occurred at the joints under loading, the overall behavior of the truss was linear, no visible deformations were recorded in the elements and joints of the truss.

ACKNOWLEDGMENTS

The authors would like to thank Civil Engineering laboratory (LGC-Annaba), Badji Mokhtar Annaba University (Annaba, Algeria) who provided facilities for conducting the various tests in the laboratory.

NOMENCLATURE

E: Young's modulus.
A: The cross-sectional area of member.
ε_i : Strain in the member.

$N_{0.Ed}$: Factored (ultimate) axial force in chord.
$N_{p.Ed}$: Factored (ultimate) axial force in chord excluding the effect of the horizontal brace force components.
β: Mean bracing width to chord width ratio $\beta = \frac{b_1 + b_2 + h_1 + h_2}{4b_0}$
z: Elastic modulus of the member.
M^i: Secondary moments.
$M_{0.Ed}$: Factored (ultimate) applied moment in plane in chord.
N_i: Axial force.
I_i: Moment of inertia.
fy_0: The yield strength of a chord member.
b_1: Compression branch width.
b_2: Tension branch width.
h_1: Compression Branch height.
h_2: Tension Branch height.
b_0: Chord width.
h_0: Chord height.
t_0: Chord thickness.
ɣ:The ratio of the chord width to twice its wall thickness.
$N_{i,Rd}$: The design value of the resistance of the joint.
k_n: Chord end stress factor for rectangular chord joints.
γ_{M5}: Partial safety factor for resistance of joints in hollow section lattice girders.
θ: Bracing angle.
$f(n)$: Function in the connection resistance formulae, which incorporate the influence of normal stresses in compression chords.
N_i^* : Connection resistance expressed as an axial force in member i.

REFERENCES

[1] Wardenier, J. (1982). Hollow section joints, Delft, The Netherlands.
[2] Slimani, F., Saidani, M., Louetri, L. (2021).Behaviour K-Joint Truss Connection with Rectangular Hollow Section. International Congress on the Phenomenological Aspects of Civil Engineering (PACE-2021), Ataturk University, Engineering Faculty, Department of Civil Engineering, Erzurum, 25030, Turkey, pp. 1–6.
[3] Slimani, F., Redjel, B., Saidani, M., Kebaili, B. (2018). Analyse expérimentale et numérique du comportement des joints des poutres en treillis métalliques de section rectangulaire creuse Experimental and numerical analysis of the behavior of the joints in rectangular hollow section trusses, Synthèse Rev. Des Sci. La Technol., 24(1), pp. 190–212.
[4] Philiastides, A. (1988).Fully overlapped rolled hollow section welded joints in trusses. PhD thesis, University of Nottingham, UK.
[5] Wardenier, J., Packer, J.A (1992). Connections between hollow sections, In Constructional Steel Design – An International Guide, Elsevier, London, UK.
[6] Tousignant, K., Packer, J.A. (2019). Analysis of rectangular hollow section trusses, Can. J. Civ. Eng., 46(3), pp. 160–175.
[7] Tousignant, K., Packer, J.A. (2015). Weld Design for Rectangular HSS Overlapped K-Connections, Eng. Journal, Am. Inst. Steel Constr., 52, pp. 259–282.
[8] Saidani, M. (1991).The effect of the flexibility of the joints on the behavior of RHS trusses. PhD thesis, Department of civil engineering, The University of Nottingham, UK, 1991.
[9] Packer, J.A., Henderson, J.E. (1992). Design guide for hollow structural section connections, 1st ed. Canadian Institute of Steel Construction, Toronto, Canada.
[10] Kim, S.-H., Lee, C.-H. (2021). Chord sidewall failure of RHS X-Joints in compression and associated design recommendations, J. Struct. Eng., 147(8), pp. 04021111, DOI: https://doi.org/10.1061/(ASCE)ST.1943-541X.0003068.

[11] Zhao, X.L., Wilkinson, T.J., Hancock, G. (2005). Cold-formed tubular members and connections: Structural behaviour and design, Elsevier.
[12] Wardenier, J., Packer, J., Zhao, X., & van der Vegte, G. (2010). Hollow sections in structural applications, (2nd ed.) CIDECT.
[13] Kouider, N., Hadidane, Y., Benzerara, M. (2022). Numerical investigation of the cold-formed I-beams bending strength with different web shapes, Frat. Ed Integrità Strutt., 16(59), pp. 153–71, Doi: 10.3221/IGF-ESIS.59.12.
[14] Guedaoura, H., Hadidane, Y. (2022). Web post-buckling strength of thin-webbed cellular beams using carbon PFRP profiles, Frat. Ed Integrità Strutt., 16(60), pp. 43–61, DOI: 10.3221/IGF-ESIS.60.04.
[15] Adel, B., Noureddine, F., Mohcene, B., Mesbah, H.A. (2020). Modeling of CFRP strengthened RC beams using the SNSM technique, proposed as an alternative to NSM and EBR techniques, Frat. Ed Integrità Strutt., 14(54), pp. 21–35, DOI: 10.3221/IGF-ESIS.54.02.
[16] Boursas, F., Boutagouga, D. (2021). Parametric study of I-shaped shear connectors with different orientations in push-out test, Frat. Ed Integrita Strutt., 15(57), pp. 24–39, DOI: 10.3221/IGF-ESIS.57.03.
[17] Bouaricha, A., Handel, N., Boutouta, A., Djouimaa, S. (2021). Load bearing capacity of thin-walled rectangular and I-shaped steel sections of short both empty and concrete-filled columns, Frat. Ed Integrità Strutt., 15(58), pp. 77–85, Doi: 10.3221/igf-esis.58.06.
[18] Behtani, A., Tiachacht, S., Khatir, T., Khatir, S., Abdel Wahab, M., Benaissa, B. (2021). Residual Force Method for damage identification in a laminated composite plate with different boundary conditions, Frat. Ed Integrità Strutt., 16(59), pp. 35–48, DOI: 10.3221/IGF-ESIS.59.03.
[19] Allaoua, F., Lebbal, H., Belarbi, A. (2021). Finite element analysis of stress state in the cement of total hip prosthesis with elastomeric stress barrier, Frat. Ed Integrita Strutt., 15(57), pp. 281–290, DOI: 10.3221/IGF-ESIS.57.20.
[20] Eurocode 3. (2003). Design of steel structures, Part 1.3 Gen. Rules Supplemary Cold Form. Thin Gauge Members Sheeting, CEN (European Commitee Standards).